The n-beam interaction brings about highly resolved ψ-scan patterns. Through this fact, we can get accurate information on the symmetry equivalence of a set of reflections and on a change in the symmetry at a structural phase transition. The high resolution is, at the same time, advantageous in checking the reliability of the goniometer and other parts of the diffractometer.

The experiment and simulation were carried out at the Centre of Advanced Instrumental Analysis, Kyushu University. The authors are indebted to Dr Y. Suemune for growing the crystal. One of the authors (AO) is grateful to Professor M. Renninger for encouragement and comments which have been given since the beginning of a series of studies on n-beam interaction, and to Dr K. Tanaka and Professor F. Mo for stimulating discussions at the International Symposium on Accuracy in Structure Factor Measurement (Warburton, Australia, 1987).

References

CHANG, S. L. (1984). *Multiple Diffraction of X-rays in Crystals*, ch. 7. Berlin: Springer.
HAUBACK, B. C. & MO, F. (1988). *Aust. J. Phys.* In the press.
LEPAGE, Y. & GABE, E. J. (1979). *Acta Cryst.* A**35**, 73–78.
LIPSON, H. & COCHRAN, W. (1953). *The Determination of Crystal Structure*, p. 32. New York: Cornell Univ. Press.
MOON, R. M. & SHULL, C. G. (1964). *Acta Cryst.* **17**, 805–812.
OKAZAKI, A., OHE, H. & SOEJIMA, Y. (1988). *Aust. J. Phys.* In the press.
OKAZAKI, A. & ONO, M. (1978). *J. Phys. Soc. Jpn*, **45**, 206–211.
OKAZAKI, A., SOEJIMA, Y. & MACHIDA, M. (1987). *J. Phys. C*, **20**, 1041–1045.
OKAZAKI, A., SOEJIMA, Y., OHAMA, N. & MÜLLER, K. A. (1985). *Jpn J. Appl. Phys.* **S24-2**, 257–259.
POST, B. (1975). *J. Appl. Cryst.* **8**, 452–456.
RENNINGER, M. (1937). *Z. Phys.* **106**, 141–176.
SOEJIMA, Y., OKAZAKI, A. & MATSUMOTO, T. (1985). *Acta Cryst.* A**41**, 128–133.
TANAKA, K. & SAITO, Y. (1975). *Acta Cryst.* A**31**, 841–845.
ZACHARIASEN, W. H. (1965). *Acta Cryst.* **18**, 705–710.

Acta Cryst. (1988). B**44**, 575–580

Structure of Barium Plutonate by Neutron Powder Diffraction

BY GARY G. CHRISTOPH,* ALLEN C. LARSON,† P. GARY ELLER,‡ JOHN D. PURSON,‡ JOHN D. ZAHRT,§ R. A. PENNEMAN‡ AND GARY H. RINEHART¶

Los Alamos National Laboratory, University of California, Los Alamos, NM 87545, *USA*

(*Received* 10 *March* 1988; *accepted* 26 *July* 1988)

Abstract

The three-dimensional crystal structure of barium plutonate, $BaPuO_3$, has been determined using Rietveld refinement of room-temperature time-of-flight neutron powder diffraction data obtained with the prototype neutron powder diffractometer (NPD) at the Los Alamos pulsed neutron facility (LANSCE). A distorted perovskite structure ($GdFeO_3$ type) is found which contains nearly regular PuO_6 octahedra with Pu—O distances of 2·2306 (5), 2·2295 (12) and 2·2230 (12) Å and unique *cis* O—Pu—O angles of 88·58 (2), 89·26 (7) and 89·59 (7)°. The PuO_6 octahedra are rotated to give Pu—O—Pu angles of 157·07 (8) and 160·53 (5)°, as compared with 180° in cubic perovskites. The observed Pu—O distances and the deviations from the cubic perovskite structure are in excellent accord with expectations based on crystal chemical models. Crystal data: $BaPuO_3$, $M_r = 427·3$, orthorhombic, *Pbnm*, $a = 6·219$ (1), $b = 6·193$ (1), $c = 8·744$ (1) Å, $V = 336·8$ Å^3, $Z = 4$. The final integrated reflection $R(F^2)$ factor is 0·034 for all reflection data from three independent detector banks. The NPD instrument and its characteristics are described.

Introduction

A large number of ABO_3 oxides adopt a structure closely related to the perovskite structure type. In the past, such materials have been investigated intensively because of their unusual magnetic and electrical properties, as well as for their interesting structural and dynamic characteristics (Galasso, 1969; Muller & Roy, 1974; Scott, 1974). Quite recently, the discovery of high-temperature superconductivity in perovskite phases has led to a gigantic resurgence of interest in their structure. Titanates (including the prototypical mineral perovskite, $CaTiO_3$) also form a basis for advanced ceramic nuclear waste forms while other perovskites, such as $BaPuO_3$, which contain transuranic and fission-product elements are relevant to nuclear waste immobilization processes (Ringwood,

* Computing and Communications Division.
† Author to whom correspondence should be directed at Los Alamos Neutron Scattering Center (LANSCE).
‡ Isotopes and Nuclear Chemistry Division.
§ Applied Theoretical Physics Division.
¶ Materials Science and Technology Division.

0108-7681/88/060575-06$03.00

Kesson & Ware, 1980; Ringwood, 1982; Williams, Morss & Choi, 1984; Morss & Eller, 1988). Thus for many reasons a detailed understanding of actinide perovskites is desirable.

Many studies of actinide perovskites have been reported over the years, yet much remains unknown. In particular, there is considerable uncertainty in the detailed understanding of the crystal structures, because characterization frequently has been based on X-ray diffraction which is relatively insensitive to small shifts in O-atom positions. It is precisely such light-atom dispositions which differentiate many of these closely related phases.

The structure of $BaPuO_3$ has been described variously as cubic and as 'pseudocubic' (Williams, Morss & Choi, 1984; Haire, 1980; Chackraburtty, Jayadevan & Sivramakrishnan, 1963; Calkin, Veryatin, Bagsyantsev & Gusev, 1975; Keller, 1962, 1972; Russell, Harrison & Brett, 1960). For the ideal (*Pm3m*) ABO_3 perovskite structure, the *B*—O—*B* linkage is precisely linear and the *B*—O bond length is one-half the unit-cell edge. For the reported cubic unit cells of $BaPuO_3$, this distance is about 2·18 Å (Fig. 1). Based on bond-length–bond-strength criteria, this distance would be about 0·06 Å shorter than the ideal value of about 2·236 Å for octahedral coordination of Pu^{IV} by oxide ions (Penneman & Eller, 1983). To allow expansion of the Pu—O distances to the empirical ideal values (Zachariasen, 1978), Penneman & Eller (1983) predicted rotation of the PuO_6 octahedra (with consequent cell-symmetry reduction). Since the ionic radii of Pu^{IV} and Pr^{IV} are very similar (Shannon, 1976; Zachariasen, 1978), we expected the observed structure of $BaPuO_3$ closely to resemble that of $BaPrO_3$, where a distortion to the orthorhombic $GdFeO_3$ structure type occurs (Jacobson, Tofield & Fender, 1972). The neutron powder diffraction study of $BaPuO_3$ described in this paper has borne out all of these predictions.

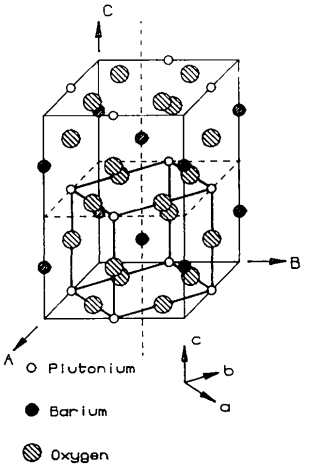

Fig. 1. A schematic view of the ABO_3 perovskite structure, showing the relationship between the ideal cubic (*Pm3m*, lower-case axes) and $GdFeO_3$-type (*Pbnm*, upper-case axes) cells.

Experimental

All preparation and handling steps were carried out with the extreme radiotoxicity of plutonium taken into account.

$BaPuO_3$ *synthesis*

Owing to the high neutron absorption cross section of the most common isotype of plutonium (mass 239), a PuO_2 substrate with the following isotopic composition was used: isotope (atom%) 238 (0·5), 239 (0·5), 240 (2·5), 214 (1·0), 242 (95·5). Plutonium dioxide (27·4 g, 0·100 mol) and $BaCO_3$ (19·7 g, 0·100 mol, Mallinckrodt Chemical Co.) were ball milled in a stainless steel container for 44 h. The mix was placed in a platinum boat and then heated in an argon atmosphere for 24 h at 1470 K to give a dark-brown solid which appeared homogeneous under microscopic examination. Furnace ramp-up and ramp-down rates of 300 K h^{-1} were used. X-ray and neutron powder diffraction patterns of the product gave sharp patterns characteristic of the $GdFeO_3$-type perovskite structure with no evidence for any other crystalline phase. The product readily and completely dissolved in 1 *M* HCl, further indicating good purity (Morss & Eller, 1988).

The neutron powder diffraction instrument

Neutron scattering experiments were performed with the prototype neutron powder diffractometer (NPD) at the Los Alamos Neutron Scattering Center (LANSCE). This instrument used a high-intensity pulsed neutron source (Windsor, 1981) and was equipped with an evacuated sample containment vessel and four banks of sixteen high-pressure ^{3}He-filled neutron detector tubes and their associated electronics. The sample center was 10·67 m from the viewed surface of the slab polyethylene moderator. The convergent beam at the sample was 1·90 cm (0·75 in) wide and 8·25 cm (3·25 in) high and bathed the entire sample. Three 'high-resolution' detector banks, each 1·0 m from the sample center and centered at $\pm 148{\cdot}3$ and $+88{\cdot}1°$ (2θ) relative to the transmitted-beam center, were made up of 30·5 cm (12 in) long by 1·27 cm (0·5 in) diameter proportional counter tubes filled with 4·0 MPa (40 atm) of ^{3}He (Reuter Stokes Co.). Data from a 'low-resolution' bank of detectors at *ca* 12° (2θ) were collected but not used in this study. The 'high-resolution' detector banks were all tilted with respect to the line from the center of the sample to the center of the banks to present constant resolution for the individual detectors within each bank. Monte-Carlo estimates including both the geometrical and temporal contributions to the resolution ($\Delta d/d$) for each of the

detector banks were: ±148·3°, 0·5%; 88·1°, 0·8%. Each bank was shielded by 10 cm (4 in) thick sodium borate-loaded paraffin wax slabs sheathed on the interior surfaces with 0·13 cm (0·050 in) thick cadmium sheet. The evacuated sample-containment vessel had incident (entrance) and diffracted (exit) beam-port windows of 0·05 cm (0·020 in) thick titanium. Diffracted-beam collimators were vertical wedges fabricated from 0·13 cm (0·050 in) thick Cd sheet and were filled with granulated B_4C. The incident- and transmitted-beam intensities were continuously monitored using low-sensitivity pass-thru ^{3}He-filled detectors. For this particular experiment, additional containment of the radioactive sample was provided by an inner evacuated vessel detailed in Fig. 2. This vessel possessed aluminium windows which were machined to 0·13 cm (0·050 in) thickness. The $BaPuO_3$ was contained in 10 cm (4 in) long by 1·27 cm (0·5 in) diameter vanadium tubes (0·025 cm wall thickness) attached to a valve by a Cu-gasketed conflat flange.

Diffraction data were collected at room temperature [298 (2) K] for 31·9 h with a proton beam current of *ca* 4 μA at 800 MeV and a pulse rate of 120 Hz. Because the detectors used are relatively insensitive to high-energy neutrons, neutrons emitted in spontaneous decay of the ^{242}Pu in the sample (approximately $1·7 \times 10^3$ neutrons $s^{-1}\,g^{-1}$ of the isotope) produced at most a weak uniform background across the time domain. With a pulsed source and with wavelength resolution by time-of-flight methods, only those emission neutrons which had become thermalized by one or more collisions would be detected by our counters. Because these neutrons would be uncorrelated with the pulse timing and thus would appear with equal likelihood in all time frames, they present no significant contribution to the net scattered neutron intensities.

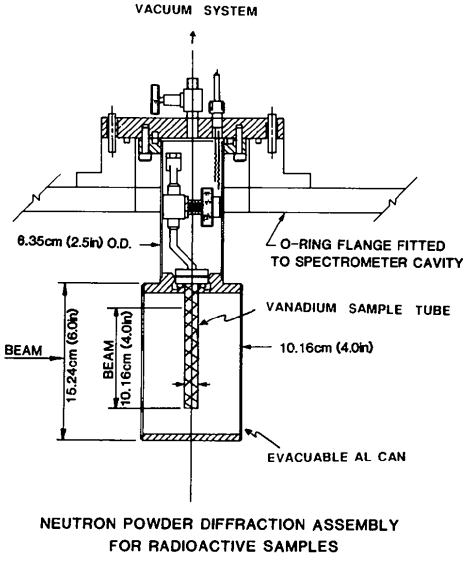

Fig. 2. Radioactive containment vessel for the neutron diffraction experiment.

Data analysis and structure solution

The time-of-flight (TOF) data from the individual detectors in each bank were binned together to form a single TOF spectrum or histogram for each bank (Von Dreele, 1984). The histograms from the three high-resolution banks comprised the input data for the Rietveld refinement of the structure (Larson & Von Dreele, 1986; Von Dreele, Jorgensen & Windsor, 1982; Rietveld, 1969). The maximum number of reflections contributing to an individual profile data point was 627. For the refinements, the incident spectrum for each bank was estimated using the scatter from a 0·62 cm (0·25 in) diameter rolled vanadium rod standard.

The structure was solved by assuming as starting parameters the cell constants and atomic coordinates for $BaPrO_3$, presumed by us to be isostructural with $BaPuO_3$. With $Z = 4$, the Ba atoms and one set of O atoms (O1) reside on 4(*c*) sites (mirror symmetry), the Pu atoms are situated on 4(*b*) sites (inversion symmetry), and the other O atoms (O2) are in general positions. Initially, only cell constants and instrumental parameters were refined. Positional and thermal parameters were introduced as the fit improved. Finally, full concurrent refinement of all the structural parameters with anisotropic thermal parameters was achieved. The diffraction data and systematic absences are consistent with space group *Pbnm* (No. 62, alternative setting of *Pnma*): $\pm(x, y, z; \frac{1}{2}-x, \frac{1}{2}+y, z; \frac{1}{2}+x, \frac{1}{2}-y, \frac{1}{2}+z; -x, -y, \frac{1}{2}+z)$, with cell constants $a = 6·219$ (1), $b = 6·193$ (1), $c = 8·744$ (1) Å, $V = 336·77$ Å^3. For comparison, the cell parameters for $BaPrO_3$ are $a = 6·181$ (1), $b = 6·214$ (1), $c = 8·722$ (1) Å, $V = 335·00$ Å^3, showing the expected close similarities of the cells (Jacobson, Tofield & Fender, 1972).* Table 1 summarizes information concerning the data used in the refinements.

The following neutron scattering lengths were used: $b_{Ba} = 0·525$, $b_O = 0·581$ and $b_{^{242}Pu} = 0·810$ fm (sears, 1986). Because the scattering length for the mixture of Pu isotopes used in the present study was not known, this length was included in the refinement as one of the variable parameters. Its final value is 0·796 (3) fm. The instrumental scale was defined at 298 (2) K using a powdered nickel standard, $a = 3·52387$ Å.

* The values of the cell parameters for $BaPuO_3$ and $BaPrO_3$ suggest that *a* and *b* are interchanged in the two structures. There is insufficient information in the paper by Jacobson, Tofield & Fender (1972) to confirm unambiguously their assignment of the *a* and *b* axes in their $BaPrO_3$ structure determination. It appears that their unit-cell constants were refined independently of the structure refinement. Interchanging *a* and *b* for $BaPrO_3$ results in an experimentally insignificant 0·1° rotation of the PrO_6 octahedra compared to the structure as reported. *Note added in proof:* Recent neutron diffraction studies at LANSCE confirm that *a* and *b* are indeed interchanged in the reported $BaPrO_3$ structure.

Table 1. *Final statistics for the three banks of neutron diffraction data used in the structure refinement of* $BaPuO_3$

The columns are: the nominal 2θ of each bank center, the d-spacing range of the data points used in the refinement, the number of individual profile data points for that bank, the number of reflections contributing to the profile, the unweighted profile R factor, $R_p = \sum[|I_o - I_c|]/\sum[I_o]$, the weighted profile R factor, $R_{wp} = \sum[w(I_o - I_c)^2]/\sum[wI_o^2]$, and the unweighted integrated reflection R factor, $R(F^2_{hkl}) = \sum|F_o^2 - F_c^2|/\sum F_o^2$.

2θ (°)	d range (Å)	Points	Reflections	R_p	R_{wp}	$R(F^2)$
+148·3	0·36–1·10	1344	4183	0·0141	0·0192	0·036
−148·3	0·36–1·10	1345	4183	0·0136	0·0184	0·033
+88·1	0·90–1·88	1220	277	0·0197	0·0274	0·024
All data	0·36–1·88	3909	8643	0·0148	0·0205	0·034

The final refinements had 60 variables including the lattice constants (3), isotropic extinction parameter (1), absorption factor (1), a scale factor for each data bank (3), a zero-point time (1), three quadratic correction terms to the total flight-path length to account for a shift in the centroid of scattering due to variation in absorption with wavelength (3), eleven background terms (4 for each 148° bank and 3 for the 88° bank), 27 atomic positional and thermal motion parameters, the Pu scattering length (1), and nine line-shape parameters.* The line-shape parameters were needed to account for differences in particle size and shape, crystallite perfection *etc.* between this sample and a standard Ni powder sample used to generate the basis values for the line shape. Table 2 summarizes the final atomic positional and thermal parameters and Table 3 contains derived interatomic distances and angles. Fig. 3 shows the fitted spectra from the 88·1° and the + and − 148·3° detector banks and Fig. 4 presents a stereoview of the structure.

The derived thermal ellipsoids for both O1 and O2 have decidely nonspherical shapes which could result from a variety or collection of causes, *inter alia* static or dynamic disorder, space-group misassignment, or an incipient phase change – all features commonly seen in perovskite structures. Near the end of the refinement procedure, we attempted to refine the structure in alternative space groups closely related to *Pbnm* and often observed in distorted perovskites. No higher-symmetry space groups (cubic, rhombohedral or tetragonal) were found to give acceptable refinement. Refinements in lower-symmetry space groups either led to divergence of the least squares or to physically unrealistic values for one or more atomic parameters. Attempts to refine disordered models were likewise unsuccessful, and such features, if present, must be too small to be pursued successfully with the present data and refinement procedure. Thus, within the limits of our data and of the powder diffraction refinement, we are confident that *Pbnm* is the correct space-group choice and that we have selected the best structural model. In any case, the apparent 'thermal motion' of the O atoms has no impact on the structural conclusions of this study. [It is interesting to note that difficulties were encountered in refining *isotropic* O-atom thermal parameters in the powder neutron diffraction study of $BaPrO_3$ (Jacobson, Tofield & Fender, 1972).]

Based on literature reports, we had expected to find one or two extraneous phases (other polymorphs or impurity metal oxides). However, the spectra were extraordinarily well fitted by assuming 100% $BaPuO_3$. Our experience with the NPD instrument has led us to expect the detection of as little as 2–3% of extraneous crystalline material.

Discussion

The neutron diffraction results clearly show that $BaPuO_3$ exists in the $GdFeO_3$-type (*Pbnm*) structure and not in the cubic perovskite structure as proposed in some earlier publications. The detailed structural features of $BaPuO_3$ are in excellent accord with expectations based on crystal chemical reasoning (Penneman & Eller, 1983), the structure being very similar to that of isostructural $BaPrO_3$. The PuO_6 octahedra are rotated by about 15° from the position in an idealized cubic perovskite to give Pu–O–Pu angles of 157·07 (8) and 160·53 (5)°, compared with the Pr–O–Pr values of 156·45 and 160·75° in $BaPrO_3$ (Jacobson, Tofield & Fender, 1972). The Pu-atom coordination is only slightly distorted from octahedral geometry, with Pu–O distances of 2·2306 (5), 2·2295 (12) and 2·2230 (12) Å and *cis* O–Pu–O angles of 88·58 (2), 89·26 (7) and 89·59 (7)°, compared with 2·22, 2·22 and 2·23 Å and 88·4, 88·6 and 89·1°, respectively, for $BaPrO_3$. The mean Pu–O distance observed in $BaPuO_3$ (2·228 Å) is very close to the expected value of 2·236 Å based on crystal chemical arguments, and probably within experimental error of uncertainties within the structural and theoretical models. The Ba atom is surrounded by twelve O atoms with a large range of Ba–O distances (2·695 to 3·532 Å, mean 3·113 Å), again very similar to that seen in $BaPrO_3$ (range 2·58–3·63 Å, mean 3·11 Å).

This work was carried out under the auspices of the US Department of Energy, Office of Basic Energy Sciences, Division of Chemical Sciences. Useful discussions with Drs E. M. Larson and R. R. Ryan are gratefully acknowledged. The availability of ^{242}Pu from the US Department of Energy's Transplutonium Element Production Program is also appreciated.

* The final least-squares refinement output and the observed neutron diffraction profile data have been deposited with the British Library Document Supply Centre as Supplementary Publication No. SUP 51168 (21 pp.). Copies may be obtained through The Executive Secretary, International Union of Crystallography, 5 Abbey Square, Chester CH1 2HU, England.

Table 2. *Final positional and thermal parameters for* $BaPuO_3$

	Site	x	y	z	U_{11}*	U_{22}	U_{33}	U_{12}	U_{13}	U_{23}
Ba	4(*c*)	0·9970 (4)	0·0134 (3)	¼	55 (5)	96 (7)	91 (5)	−24 (6)	0	0
Pu	4(*b*)	0	½	0	11 (3)	34 (4)	23 (3)	12 (5)	9 (4)	14 (4)
O1	4(*c*)	0·0703 (3)	0·4884 (5)	¼	103 (6)	243 (10)	12 (5)	17 (7)	0	0
O2	8(*d*)	0·7275 (2)	0·2719 (2)	0·0368 (1)	115 (5)	106 (5)	180 (5)	−98 (3)	30 (4)	−31 (5)

*The U_{ij} values are multiplied by 10^4 and are defined by $T = \exp\{-2\pi^2[U_{11}h^2a^{*2} + U_{22}k^2b^{*2} + U_{33}l^2c^{*2} + 2(U_{12}hka^*b^* + U_{13}hla^*c^* + U_{23}klb^*c^*)]\}$.

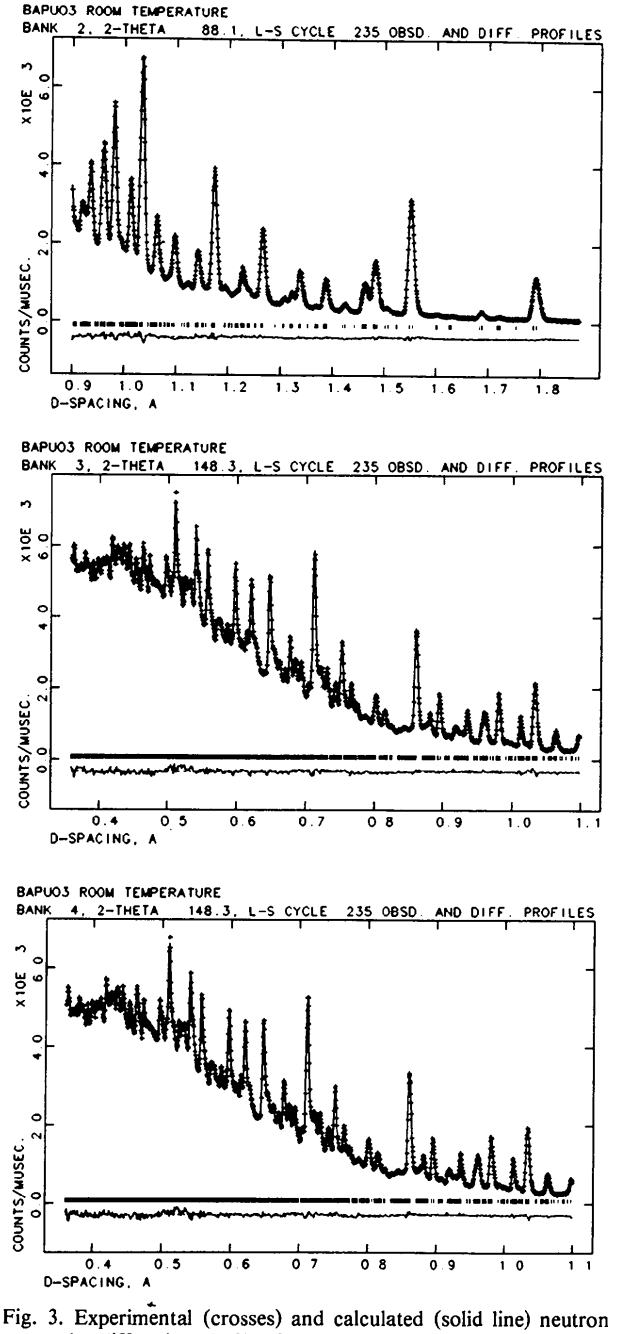

Fig. 3. Experimental (crosses) and calculated (solid line) neutron powder diffraction profiles for $BaPuO_3$. Reflection positions are indicated by ticks and the lower curve is the difference profile. Data shown are for the 88·1 and the ±148·3° detector banks.

Table 3. *Derived unique interatomic distances* (Å) *and angles* (°) *for* $BaPuO_3$

Pu–O1 (×2)	2·2306 (5)	O1–Pu–O2	89·26 (7), 89·59 (7)
Pu–O2 (×2)	2·2295 (12)	O2–Pu–O2	88·58 (2)
Pu–O2 (×2)	2·2230 (12)	Pu–O1–Pu	157·07 (8)
Ba–O1	2·695 (3)	Pu–O2–Pu	160·53 (5)
Ba–O1	2·977 (4)		
Ba–O1	3·283 (3)		
Ba–O1	3·531 (3)		
Ba–O2l(×2)	2·768 (2)		
Ba–O2 (×2)	2·974 (2)		
Ba–O2 (×2)	3·181 (2)		
Ba–O2 (×2)	3·514 (2)		

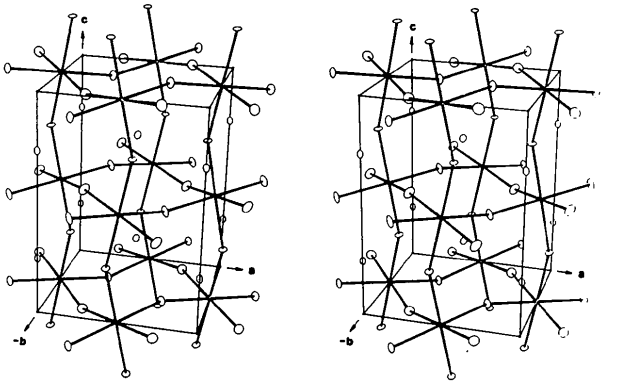

Fig. 4. Stereoview of the $BaPuO_3$ structure.

References

CALKIN, N. P., VERYATIN, V. S., BAGSYANTSEV, V. F. & GUSEV, V. F. (1975). *Radiokhimiya*, **17**, 604–608. (English translation).

CHACKRABURTTY, D. M., JAYADEVAN, N. C. & SIVRAMAKRISHNAN, C. K. (1963). *Acta Cryst.* **16**, 1060–1061.

GALASSO, F. S. (1969). *Structure, Properties, and Preparation of Perovskite-Type Compounds*. New York: Pergamon Press.

HAIRE, R. G. (1980). *Proc. 10th Journée des Actinides*, p. 19.

JACOBSON, A. J., TOFIELD, B. C. & FENDER, B. E. F. (1972). *Acta Cryst.* B**28**, 956–961.

KELLER, C. (1962). *Nucleon*, **4**, 271–277.

KELLER, C. (1972). *MTP Review of Science, Inorganic Chemistry*, Ser. 1, Vol. 5, edited by K. W. BAGNALL, pp. 47–85. London: Butterworths.

LARSON, A. C. & VON DREELE, R. B. (1986). *Generalized Crystal Structure Analysis System*. Report LAUR-86-748. Los Alamos National Laboratory, NM, USA.

MORSS, L. R. & ELLER, P. G. (1988). *Radiochim. Acta*. Submitted.

MULLER, O. & ROY, R. (1974). *The Major Ternary Structural Families*. New York: Springer-Verlag.

PENNEMAN, R. A. & ELLER, P. G. (1983). *Radiochim. Acta*, **32**, 81–87.

RIETVELD, H. M. (1969). *J. Appl. Cryst.* **2**, 65–71.

RINGWOOD, A. E., KESSON, S. E. & WARE, N. G. (1980). *Sci. Basis Nucl. Waste Manage.* **2**, 265–272.
RINGWOOD, T. (1982). *Am. Sci.* **70**, 201–207.
RUSSELL, L. E., HARRISON, J. D. L. & BRETT, N. H. (1960). *J. Nucl. Mater.* **2**, 310–320.
SCOTT, J. F. (1974). *Rev. Mod. Phys.* **46**, 83–128.
SEARS, V. F. (1986). *Methods Exp. Phys.* **23A**, 521–550.
SHANNON, R. D. (1976). *Acta Cryst.* A**32**, 751–767.
VON DREELE, R. B. (1984). Personal communication.
VON DREELE, R. B., JORGENSEN, J. D. & WINDSOR, C. G. (1982). *J. Appl. Cryst.* **15**, 581–589.
WILLIAMS, C. W., MORSS, L. R. & CHOI, I. (1984). *Am. Chem. Soc. Symp. Ser.* No. 246, edited by G. S. BARNEY, J. D. NAVRATIL & W. W. SCHULTZ, pp. 323–334. Washington, DC: American Chemical Society.
WINDSOR, C. G. (1981). *Pulsed Neutron Scattering*. New York: Halsted Press.
ZACHARIASEN, W. H. (1978). *J. Less-Common Met.* **62**, 1–7.

Acta Cryst. (1988). B**44**, 580–585

Electron-Density Distribution in Crystals of Dipotassium Tetrachloropalladate(II) and Dipotassium Hexachloropalladate(IV), $K_2[PdCl_4]$ and $K_2[PdCl_6]$ at 120 K

BY HIROYUKI TAKAZAWA, SHIGERU OHBA AND YOSHIHIKO SAITO

Department of Chemistry, Faculty of Science and Technology, Keio University, Hiyoshi 3, Kohoku-ku, Yokohama 223, Japan

(*Received* 1 *June* 1988; *accepted* 9 *August* 1988)

Abstract

Mo $K\alpha_1$, $\lambda = 0.70926$ Å, $T = 120$ (2) K. (I): $K_2[PdCl_4]$, $M_r = 326.4$, tetragonal, $P4/mmm$, $a = 7.0259$ (3), $c = 4.0797$ (2) Å, $V = 201.39$ (2) Å^3, $Z = 1$, $D_x = 2.69$ Mg m^{-3}, $\mu = 4.55$ mm^{-1}, $F(000) = 151.7$, final $R = 0.021$ for 893 unique reflections. (II): $K_2[PdCl_6]$, $M_r = 397.3$, cubic, $Fm3m$, $a = 9.6374$ (4) Å, $V = 895.12$ (7) Å^3, $Z = 4$, $D_x = 2.95$ Mg m^{-3}, $\mu = 4.71$ mm^{-1}, $F(000) = 744.0$, final $R = 0.011$ for 393 unique reflections. The Pd—Cl bond lengths are 2.3066 (2) and 2.3094 (3) Å for (I) and (II), respectively. The asphericity of the 4*d* electron distribution in the square-planar and octahedral Pd complexes could be detected clearly. Above and below the $[PdCl_4]^{2-}$ plane of (I), excess densities of 2.3 (3) e Å^{-3} are found at 0.47 Å from the Pd nucleus, suggesting enhancement of the d_{z^2} orbital population. In (II), positive deformation densities corresponding to the t_{2g} orbitals are observed in the [111] directions at 0.5 Å from the Pd nucleus and 1.4 (3) e Å^{-3} in height. These charge asphericities could be reproduced by the multipole expansion method with reasonable *d*-orbital populations.

Introduction

Since Iwata & Saito (1973) reported the aspherical distribution of the 3*d* electrons in $[Co(NH_3)_6][Co(CN)_6]$, a number of studies on transition metals and their complexes have been performed (Coppens & Hall, 1982; Toriumi & Saito, 1983). Preliminary papers on $K_2[PtCl_4]$ (Ohba, Sato, Saito, Ohshima & Harada, 1983) and $K_2[PtCl_6]$ (Ohba & Saito, 1984) suggested that even 5*d* electrons may be detected in spite of a very small valence/total electron ratio. Before exploring further the asphericity of 5*d* electrons in a ligand field, the isomorphous Pd complexes involving 4*d* electrons were examined in the present study.

Experimental

(I): Dark-green needle-like crystals were grown from an aqueous solution of $PdCl_2$ and KCl. A crystal was shaped into a sphere of 0.378 (5) mm in diameter and cooled with a stream of cold nitrogen gas. Intensities were measured on a Rigaku AFC-5 automated four-circle diffractometer with graphite-monochromatized Mo $K\alpha$ radiation, θ–2θ scan technique with scan speed 6° min^{-1} in θ and scan width $(1.4 + 0.36\tan\theta)°$. Range of indices, $-12 \le h$, $k \le 12$, $0 \le l \le 7$ ($0 < 2\theta \le 80°$); $-17 \le h \le 17$, $0 \le k \le 17$, $0 \le l \le 9$ ($80 < 2\theta \le 120°$). Standard reflections varied within 3%, 4753 reflections were measured; 4387 reflections observed with $|F_o| > 3\sigma(|F_o|)$; 893 unique reflections ($R_{int} = 0.016$). Lattice constants were based on 20 2θ values ($60 < 2\theta < 76°$). Correction for absorption made with $\mu r = 0.860$ ($0.293 < A < 0.351$). Conventional refinement performed by the full-matrix least-squares program *RADIEL* (Coppens, Guru Row, Leung, Stevens, Becker & Yang, 1979). Function $\sum w(|F_o| - |F_c|)^2$ minimized with weight $w^{-1} = \sigma^2(|F_o|) + (0.015|F_o|)^2$. Introducing an isotropic secondary-extinction correction parameter (Zachariasen, 1967), $g = 0.14\,(1) \times 10^{-4}$, reduced R from 0.030 to 0.021 for 893 unique reflections. $wR = 0.036$, $S = 1.9$, reflection/parameter = 81.2, $\Delta/\sigma < 0.2$. Complex neutral-atom scattering factors were taken from *International Tables for X-ray Crystallography* (1974). Calculations were carried out on a FACOM M-380R computer of this university.

0108-7681/88/060580-06$03.00